Molecular dynamics simulations of supercooled and amorphous $Co_{100-x}Zr_x$: Atomic mobilities and structural properties

U. K. Rößler* and H. Teichler
Institut für Materialphysik der Universität Göttingen and SFB 345, Hospitalstrasse 3/5, D-37073 Göttingen, Germany
(Received 1 July 1999)

Molecular dynamics simulations are reported on $Co_{100-x}Zr_x$ in the complete range of compositions. The simulations are based on Hausleitner-Hafner potentials. For the glassy states of the alloys, a comparison of simulated pair-correlation functions with experimental data is presented. Diffusivities were evaluated for the liquid and supercooled melt from isothermal simulation runs. Therefrom a strong dependency on alloy composition is found for the critical temperature $T_c(x)$ of the mode-coupling theory. Lines of constant averaged diffusivity in the supercooled melts scale closely with this temperature. The ratio of the component diffusivities shows a more involved variation with temperature and composition. These variations reflect differences in the amorphous structure of the alloys, which are quantified in terms of the chemical short-range-order at the level of tetrahedral clusters.

PACS number(s): 61.20.Ja, 61.25.Mv, 64.70.Pf

I. INTRODUCTION

The liquid-glass transition [1] is one of the unsolved open questions in current condensed matter physics. It seems primarily of dynamical origin and is related to a significant slowing-down of the undercooled liquid's dynamics until structural arrest is reached. In the range of undercooled liquids, the behavior is well described, e.g., by the mode-coupling theory (MCT) [2–5] for dense liquids. So far, the theory was worked out for idealized systems such as soft-sphere [6], and hard-sphere [7,8] models or Lennard-Jones systems [9,10]. More recently, glass transitions of systems of rigid linear molecules were treated by MCT [11–13], and attempts at formulations for arbitrary molecules have been made [14,15]. For glass-forming metallic alloys, any theoretical information is missing at present, how, in the case of real systems, parameters such as the chemical composition determine the transition and the transition temperature. Composition effects are of particular interest in the field of metallic glasses due to the wide range of miscibility of the components and their partial immiscibility in crystalline phases. Thus, the question arises, how these properties affect the glass forming ability. There is a strong interest in composition effects of metallic glass formers due to the recent development of the unique class of ''bulk'' metallic glasses by Inoue [16] and Johnson [17]. These materials are ternary or multicomponent metallic alloys, which show their extraordinary thermal stability with respect to crystallization in a restricted range of composition only [18,19]. Within this range glass-forming ability and glass temperature vary systematically. Thus, an understanding of compositional effects is called for to understand the stability of different glassy metals.

In the present study we investigate the composition dependence of viscous flow and atomic motion in undercooled metallic glass-forming liquids by means of molecular dynamics (MD) simulations. To investigate such problems, MD simulations are well suited as in the metallic liquids the equilibration and sampling over the relevant part of the configuration space takes place in times currently well accessible to this method so that representative stationary situations can be analyzed. Here, the slowing down of the atomic motions can be viewed as a signature of the approach to the glass transition. The present exploratory study considers the $Co_{100-x}Zr_x$ system as a typical example of a binary transition-metal glass. The binary system was chosen to keep the situation as simple as possible. $Co_{100-x}Zr_x$ was selected as this system and related Zr-based glass-forming alloys have been extensively studied by experiments [20]. Moreover, there exist suitable interatomic potentials provided by Hausleitner and Hafner through their ''hybridized nearly-free-electron tight-binding-bond'' (NFE-TBB) description of the interatomic couplings. The approach allows reliable modeling of this amorphous binary system and similar ones in MD simulations. Hausleitner and Hafner [21–23] have successfully demonstrated that with their NFE-TBB model in particular the structural and electronic properties of binary $(Fe,Co,Ni)_{100-x}Zr_x$ glasses can be realistically simulated as well as their magnetic properties including a-$Co_{100-x}Zr_x$ [24].

The paper is organized as follows. Section II presents briefly the model and method of our simulations and Sec. III presents the results. First a comparison between experimental structure data for a-CoZr alloys with our simulated configurations is given. The slowing down of the averaged diffusivities as measure of viscous flow in the supercooled liquids is investigated in Sec. III B. In Sec. III C, additional simulations of the relaxation behavior of the supercooled liquids at two different compositions are presented. Section III D yields the results about the ratio of the component diffusivities. Section III E describes the structure of a-$Co_{100-x}Zr_x$, providing a detailed quantification of the chemical short-range-order (SRO) of liquid and amorphous

*Present address: IFW Dresden, Institut für metallische Werkstoffe, Postfach 270016, D-01171 Dresden, Germany. Electronic address: u.roessler@ifw-dresden.de

$Co_{100-x}Zr_x$. This description is employed in Sec. IV to discuss the differences in the behavior of the component diffusivities.

II. INTERACTION-MODEL AND PREPARATION OF THE AMORPHOUS CONFIGURATIONS

The simulations were performed using Hausleitner-Hafner potentials for $Co_{100-x}Zr_x$ calculated by the same methods as described in Ref. [22]. To simplify the application of these pair potentials, which depend on alloy composition and volume, we consider (N,V,T) ensembles in the present study. The MD simulations are carried out using a fifth order Gear-predictor-corrector algorithm [25] with a time step $\Delta t = 2.0\times 10^{-15}$ s and periodic boundary conditions. The alloy volumes were calculated from the phenomenological Miedema theory [26], which gives good estimates for the experimental volume of glasses of these alloys [27]. It may be pointed out here that according to our tests a rescaling of the volume by a few percent does not change the resulting amorphous packing. Hence, the limitation to fixed volume seems justified in the simulations. For resolving the composition dependence sufficiently, we studied a sequence of systems with increasing Zr concentration in steps of 5 at. % or less with $N=648$ particles each. The samples for each composition were prepared independently by a quenching process starting at 3000 K. At this temperature the samples were homogenized over 57 600 time steps and then quenched at a rate of 2.6×10^{13} K/s. Starting configurations for isothermal runs were stored during the simulated quench. For several compositions we compared results for the structural properties with additional runs with $N=5184$. Within the accuracies achieved, pair-correlation functions and chemical SRO parameters, as defined below in Sec. III D, did not differ for the larger samples from those of the small samples. Hence, we restricted further investigations to the small samples.

III. RESULTS

A. Pair-correlation functions

For several temperatures, we sampled pair-correlation functions from isothermal runs. Figure 1 presents a comparison of our simulated data with the experimental x-ray diffraction results for *a*-CoZr at higher contents of Zr [27]. In Figs. 2 and 3, we compare simulated static structure factor and partial pair-correlation functions for $Co_{90}Zr_{10}$ with results from a recent combined x-ray diffraction and EXAFS study [28]. The resolution of these methods seems unable to resolve any structure of the Zr-Zr pair correlations because of the low contribution of these pairs of minority atoms in this alloy. However, the majority Co-Co pair correlations are well described by the simulation results. Generally, the agreement between simulation results and both sets of experimental data is satisfactory and comparable to that reported by Hausleitner and Hafner for their MD simulations for the $Ni_{100-x}Zr_x$ [22] and the $Fe_{100-x}Zr_x$ [23] system. Especially, the trends of the subpeaks in the first main peak of $G(r)$ shown by the experimental data are fairly well reproduced by the simulated configurations. Thus, our model is consistent with present experimental information regarding the chemical SRO in the (composite) nearest-neighbor (NN) shells and the changes in composition of this shell with composition of the alloy.

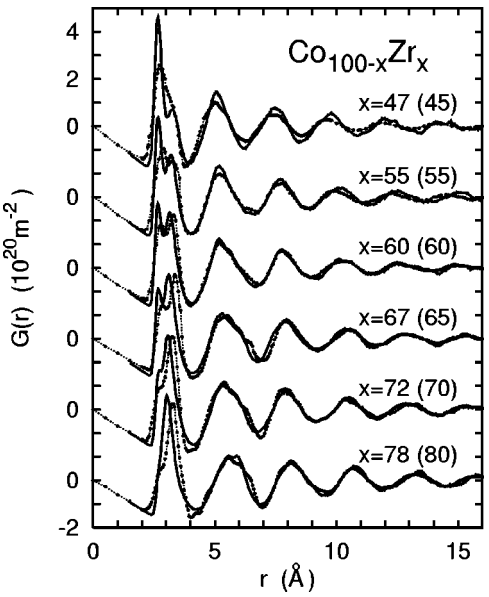

FIG. 1. Total reduced pair-correlation functions $G(r)$ weighted with x-ray visibilities for a-$Co_{100-x}Zr_x$. Comparison of experimental data with simulation results. Dots joined by dotted lines: experimental data from Ref. [27]. Full lines: simulation results sampled at 300 K. The simulation data refer to alloys with concentrations x given in brackets.

B. Averaged atomic mobilities

Here we report results on average mobilities at different alloy compositions obtained from isothermal MD runs. The averaged mobility considered in this subsection is the concentration weighted diffusion coefficient of the two species $D=(1-x)D_{Co}+xD_{Zr}$. In the liquid state with dominating viscous flow, which is characterized by a continuous move-

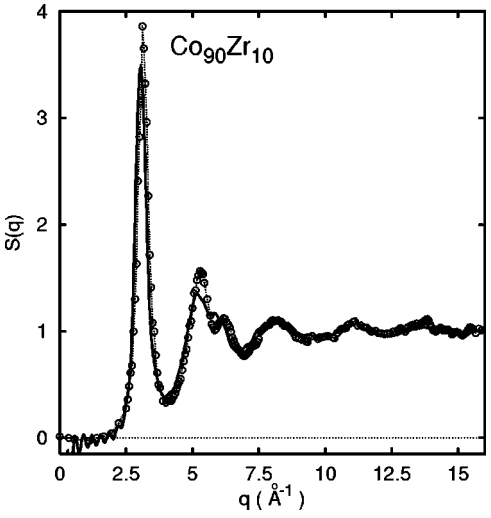

FIG. 2. Simulation results of static structure factor $S(q)$ (full line) for $Co_{90}Zr_{10}$ at 300 K compared to experimental results (circles joined by dotted line) from x-ray diffraction by Babanov *et al.* [28].

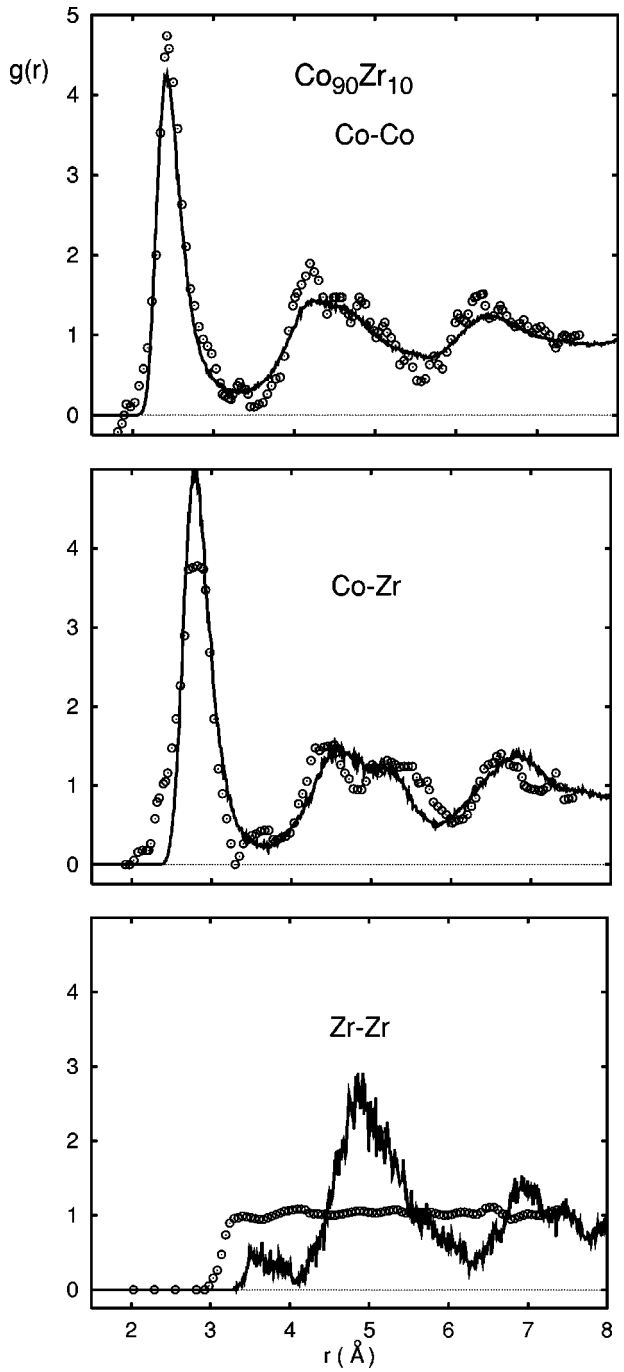

FIG. 3. Comparison of simulated partial pair-correlation functions (full lines) for $Co_{90}Zr_{10}$ at 300 K to experimental pair-correlation functions derived from x-ray diffraction and EXAFS measurements [28] (open circles).

ment of all atoms, it is reasonable to consider averaged diffusivities for the alloys first. The diffusivities may be calculated directly from the mean-square displacements

$$D=\lim_{t\to\infty}\frac{(1/N)\sum_{i=1}^{N}|\mathbf{x}_i(t)-\mathbf{x}_i(0)|^2}{6t}, \tag{1}$$

where $\mathbf{x}_i(t)$ are the coordinates of atom i at time t, and N is the number of atoms. The component diffusivities, which will be investigated later, are calculated similarly by restricting the summation in Eq. (1) to atoms of the particular type.

D was sampled as function of temperature for various alloy compositions from sequences of several isothermal MD runs over 72 or 144 ps. Each sequence started with a configuration stored during the quenching simulation at temperatures in the interesting temperature range. Over those time intervals the extrapolation according to Eq. (1) becomes sufficiently stable as long the temperature is well above glass transition. We performed at least 8 up to more than 20 consecutive runs at each temperature, which amounts to simulation times between 0.5 to 1.5 ns. In the melt, the consecutive isothermal runs are independent of elapsed simulation time as, there, the atoms are still highly mobile, thus ensuring an efficient sampling of configuration space. Only at low temperatures around glass-transition, we find a drift in the diffusivities D calculated for consecutive runs. This drift to lower values with the number of runs indicates irreversible relaxation processes taking place on a slower time scale. We stress here, that we focus our attention solely to higher temperatures in the proper supercooled state, where equilibrium is reached within simulation time. The data for $D(T)$ are the averages for the consecutive isothermal runs.

To quantify our results for the temperature dependency of the diffusivities, we invoke a critical law

$$D(T)=b(T-T_c)^{\gamma}. \tag{2}$$

Such a critical fit for diffusivities from MD data [29] was applied previously for hard-sphere systems in the context of mode-coupling theory [3]. In that theory, the temperature T_c marks a dynamical transition in the supercooled state, which takes place above the glass temperature T_g and triggers the structural arrest as dynamics slows down dramatically around T_c. The link of the critical law applied to fit $D(T)$ with the MCT should not be overstressed. Bosse and Kaneko find in their evaluation of the full q-dependent MCT for binary mixtures of hard spheres [8] that such a critical law does not arise naturally. However, Bosse and Kaneko find that the slowing down of component diffusivities of a mixture of hard spheres, described by their theory, can be fitted by a critical law. Usually, it is assumed that T_g is in the range of about 15% below T_c. Here, we only apply the critical fits as a comfortable characterization for the complete surface $D(x;T)$. Thus, we do not attempt a quantitative verification of theoretical predictions about the dynamics close to glass transition. An investigation at those lower temperatures and a quantitatively reliable determination of T_g would require far longer simulation times [30,31]. A choice of our MD data for $D(T)$ is given in Fig. 4 in an Arrhenius plot, along with the corresponding critical fits. They clearly display a systematic deviation from a pure Arrhenius behavior.

Figure 5 demonstrates the quality of the critical fits for $Co_{50}Zr_{50}$. In this plot the bending of the curve D as function of temperature around $T_c=1090$ K is clearly found. The inset of Fig. 5 shows the effect of restricting the upper bound of the temperature interval $[T_c, T_{\max}]$ used for the critical fit. For intervals large enough, T_c may be fixed to about $\pm$ 50 K. However, the critical exponent γ cannot be fixed by this method better than in the interval between 1.4 and 2. This is not surprising as the variation of D covers only about three

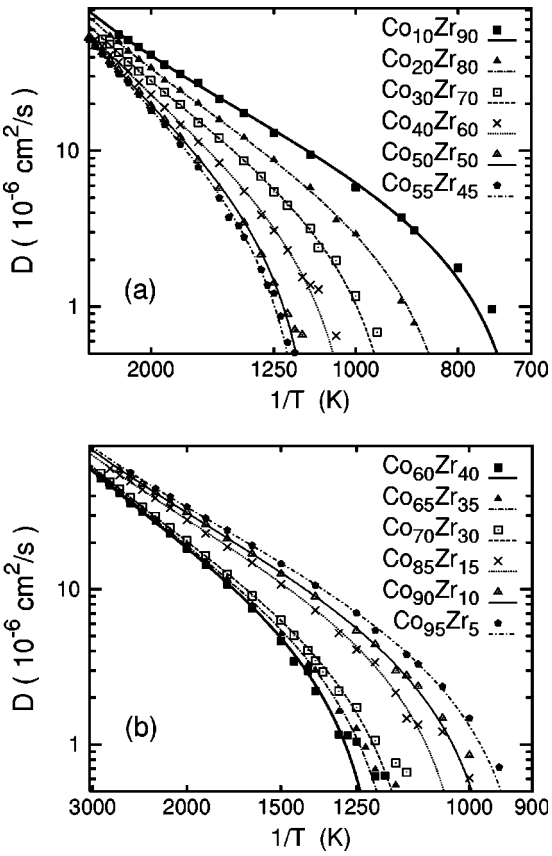

FIG. 4. (a) and (b) Arrhenius plot for averaged diffusivities D in supercooled alloys $Co_{100-x}Zr_x$ at different concentrations as indicated in the figures. Symbols refer to isothermal MD runs; lines are critical fits to these data according to Eq. (2).

decades in the given temperature interval. If this interval is chosen too small almost any value $3.5>\gamma>1.4$ could be found as is seen by the breakdown of the fit for $T_{\max}<1500$ K. Thus, γ has only limited meaning for present study. If one uses the same interval $[T_c, T_c+\text{const}]$ for all alloys the systematic variation of T_c with alloy composition may still be assessed satisfactorily. This is the method we

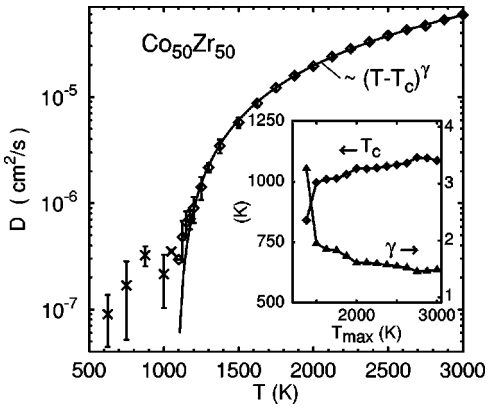

FIG. 5. $D(T)$ for $Co_{50}Zr_{50}$. Symbols refer to averages of $D(T)$ from sequences of isothermal runs, errorbars indicate the corresponding errors. The line is a critical fit to all data with $T>T_c(\diamond)$. The inset shows the behavior of the fitting-parameters when restricting the interval of data points in the fit to $[T_c, T_{\max}]$ with varying $T_{\max}$.

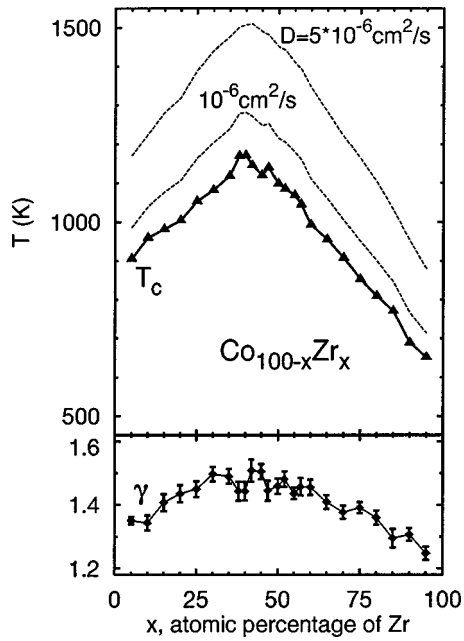

FIG. 6. $T_c(x)$ and $\gamma(x)$. Parameters of the critical fits [Eq. (2)] to the averaged diffusivities as function of alloy composition x. (Symbols refer to results for the different alloys. Lines are guide to the eye.) The error bars given for $\gamma(x)$ refer to a 68.3% confidence interval from the fitting. Corresponding errors of T_c are less than ± 20 K. The two dashed lines indicate the temperatures with $D(x)=\text{const}$ with the given values.

used to calculate the values $T_c(x)$ and $\gamma(x)$ presented in Fig. 6.

We find a rather smooth variation of $T_c(x)$, with an increase from 900 to 1170 K in the interval $5\leqslant x\leqslant 38$ atomic percentage of Zr, and a decay for alloys with atomic precentage of Zr $x\geqslant 40$ reaching $T_c(95)=650$ K. This huge variation over 500 K in T_c is a prominent feature of our results. When comparing the diffusivities close above T_c in different alloys, we find that the temperatures, where a fixed value of D is reached, closely follow $T_c(x)$ (see Fig. 6). This implies that the function may be rescaled with $T_c(x)$, so that $D(x;T-T_c)\simeq\text{const}$.

These results assert that the slowing down of diffusivities in the supercooled state is insensitive to details in the microscopic structure of the amorphous packings. Therefore, a unifying approach based, e.g., on hydrodynamic ideas may be qualitatively justified from these results. However, closer inspection reveals certain interrelations between the slowing down and the structural properties of the alloys at different composition. This is the subject of Secs. III D and III E below.

C. Decay of density-density correlations

Recent studies about the glass transition in MD-simulated systems aimed at testing predictions of MCT have provided detailed insights in the change of the dynamics close to the glass transition, respectively close to the critical temperature T_c [30–35]. The central quantities of these studies are density-density correlation functions. For two different CoZr alloys we performed similar calculations to check the relation between the slowing down of the mobilities of the atoms

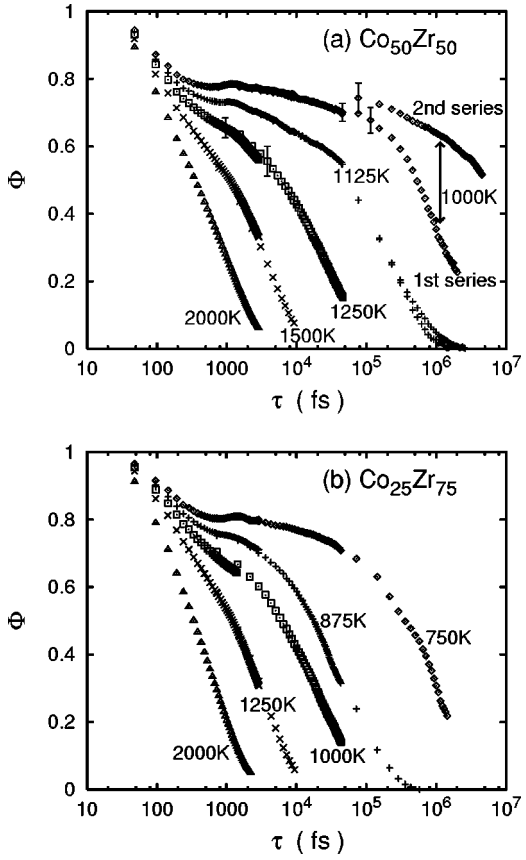

FIG. 7. (a) and (b) Self-part of the intermediate scattering function $\Phi(\tau)$ [Eq. (3)] at different temperatures. (a) $Co_{50}Zr_{50}$ (wave vector $|\mathbf{q}|=2.28$ Å^{-1}). For the longest time intervals τ around 10^6 fs two series are given for $T=1125$ K and $T=1000$ K. For the latter temperature, the two series display significant aging effects indicated in the figure. Corresponding critical temperature: $T_c^D=1090$ K (see Fig. 6). (b) $Co_{25}Zr_{75}$ (wave vector $|\mathbf{q}|=2.15$Å^{-1}), critical temperature $T_c^D=850$ K.

and the much more detailed information from the decay of these time-correlation functions. In this section, we will denote the critical temperatures from the critical fits to $D(T)$ as T_c^D. The runs are also carried out in the (N,V,T) ensemble, using the relaxed configurations from the previous isothermal runs as starting configurations. The simulation times needed were considerably longer than the evaluation of $D(T)$ in the supercooled region, reaching to about 10 ns. However, no very long simulation runs over many nanoseconds have been attempted as in Refs. [30,31], which were necessary to investigate the behavior close to T_c in detail.

We follow the prescription for such simulations given in Ref. [31] studying the self-part of the intermediate scattering function:

$$\Phi(\tau)=\langle\langle\exp\{i\mathbf{q}\cdot[\mathbf{x}_i(\tau+t)-\mathbf{x}_i(t)]\}\rangle\rangle, \tag{3}$$

where the double brackets denote averages with respect to the number of particles and times t. Φ is evaluated for the star of wave vectors pointing in the direction of the edges of the simulation box with sidelength L, i.e., $\mathbf{q}=(2\pi/8L,0,0)$ and permutated. Thus, the density fluctuations with wavelength of about the interparticle distances are tested.

Figure 7 shows Φ for (a) $Co_{50}Zr_{50}$ and (b) $Co_{25}Zr_{75}$. The series for the short time intervals have been generated after the series for the longest time intervals in the simulations for both alloys. Φ displays a typical two-step decay for the simulated undercooled melts around the critical temperature T_c^D. When decreasing the temperature below T_c^D, a strong increase of the final relaxation time takes place. The resulting plateau in Φ is typical for the onset of structural arrest. It stretches over about one decade in τ in the first simulation sequences for both alloys. In the case of $Co_{50}Zr_{50}$ we performed a second series of simulations using as starting conditions the better relaxed configurations of the first series of runs at the same temperature. Therefrom, we again evaluated $\Phi(\tau;T)$ for the long time-intervals also shown in Fig. 7(a). For $T=1125$ K, i.e. above T_c^D, both series coincide within the statistical errors. On the other hand, at $T=1000$ K, that means below T_c^D, strong aging effects are visible as expected below the critical temperature: The plateau now extends to considerably longer times [see Fig. 7(a)]. Thus, the temperature T_c^D determined from diffusivities is a consistent estimate of the critical temperature T_c predicted by the mode-coupling theory [3,8] for the change of the overall relaxation behavior of $\Phi(\tau;T)$.

Comparing present results about $\Phi(\tau;T)$ to our experiences about the behavior of simulated supercooled metallic liquids from far better relaxed simulations for $Ni_{50}Zr_{50}$ [31,32], we may conclude that the $T_c^D(x)$ are reliable measures to fix the temperatures, where viscous flow in the supercooled melts breaks down. Additionally, recent simulations on polymer melts have shown that T_c may be fixed rather accurately without reaching equilibrium, i.e., without achieving stationarity of the dynamics as measured by time correlation functions [36].

D. Ratio of the component diffusivities

If we restrict summation in definition (1) to either Co or Zr atoms we may calculate diffusivities for the alloy components. A critical fit for $D_{\mathrm{Co}}(T)$ and $D_{\mathrm{Zr}}(T)$ may be performed in the same way. The difference in the mobilities of the alloy components close to T_c may be best understood by their ratio

$$\zeta(T)=D_{\mathrm{Co}}^{\mathrm{fit}}(T)/D_{\mathrm{Zr}}^{\mathrm{fit}}(T) \tag{4}$$

with component diffusivities $D_{\mathrm{Co,Zr}}^{\mathrm{fit}}(T)$ calculated from the critical fits. ζ enables an extrapolation of the viscous behavior of the two alloy components to temperatures close to T_c. Calculating this ratio directly from isothermal MD runs close to T_c is not satisfactory because any irreversible relaxation process in that range of temperature should induce movements of both components which would tend to hide the differences in their dynamics due to viscous flow. In Fig. 8 the dependence of ζ on x along lines with $T=T_c+\mathrm{const}$ is displayed.

At high temperatures $T\geqslant T_c+500$ K, ζ varies between 1 and 2, thus viscous flow is marked by closely coupled motions of Co and Zr atoms with slightly higher mobility of Co atoms. At lower temperatures, we may distinguish three different types of alloys by different behavior of the respective ζ. For atomic percentage of Zr $x\leqslant 40$, we find a steep increase of ζ when lowering the temperature. This means a

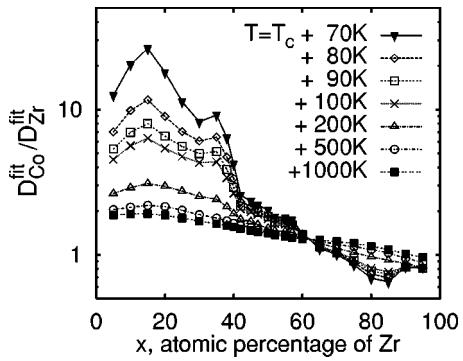

FIG. 8. Ratio of the component diffusivities $\zeta = D_{\mathrm{Co}}^{\mathrm{fit}}/D_{\mathrm{Zr}}^{\mathrm{fit}}$ for alloys $\mathrm{Co}_{100-x}\mathrm{Zr}_x$ at different temperatures $T = T_c + \mathrm{const.}$ (Lines are guide to the eye.)

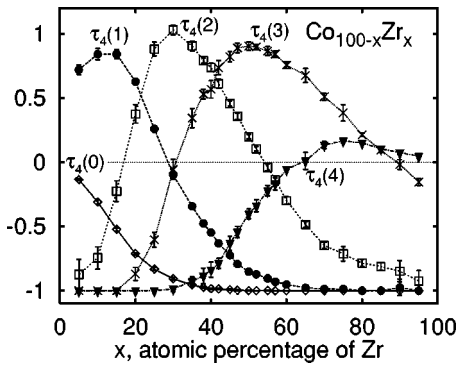

FIG. 9. Chemical SRO-order parameters τ_4 for tetrahedral clusters as functions of alloy composition [see definition Eq. (5)]. Positive values of $\tau_4(n)$ mean a surplus, negative values a deficiency of the corresponding tetrahedral cluster $\mathrm{Co}_{4-n}\mathrm{Zr}_4$ in the amorphous structure of the alloy. The parameters have been sampled at $T = 1250$ K.

high mobility of the Co atoms relative to the mobility of Zr. In the interval $40 \leqslant x \leqslant 60$, the mobility of the two alloy components seems to be closely coupled, still. We find a slight increase of ζ close to T_c, however, with values of ζ around 2. The Zr-rich alloys, $x \geqslant 60$, show the opposite behavior: ζ decreases when approaching T_c. Hence, in the Zr-rich alloys, the smaller component Co seems to own a lower mobility than the larger species Zr.

E. Chemical ordering: Tetrahedral clusters

To understand the behavior of ζ, we consider the differences in the amorphous structures of the different alloys. We will discuss these differences by an analysis of the chemical short-range order of the amorphous structures in terms of the probabilities for finding chemically different local clusters in the simulated models. First, neighbouring atoms are defined by partial cutoff radii for the different pairs of alloy components. We define these radii as the location of the first minima following the first maxima in the partial pair-distribution functions $4\pi r^2 g_{XY}(r)$ for the different alloys.

Now, we may define a quantitative measure for the SRO in the packings, which goes beyond pair correlations. When we count the numbers of chemically different tetrahedral clusters $\mathrm{Co}_{4-n}\mathrm{Zr}_n$, $n = 0, \ldots, 4$, by $N_4(n)$ a set of order-parameters may be defined by

$$\tau_4(n) = \frac{N_4(n)}{\binom{4}{n} c_{\mathrm{Co}}^{4-n} c_{\mathrm{Zr}}^{n} \sum_{n'} N_4(n')} - 1 \quad . \tag{5}$$

The denominator in the fraction counts the probability to find a certain tetrahedral cluster in an alloy if Co and Zr atoms would be entirely interchangeable. $\tau_4(n) = 0$ for all n means that no chemical ordering is present in the packing at the level of tetrahedral NN clusters. If $\tau_4(n) > 0$ for a particular n, then there is a statistically significant surplus of the corresponding tetrahedral cluster $\mathrm{Co}_{4-n}\mathrm{Zr}_n$. If $\tau_4(n) < 0$ there is a deficiency of that cluster. Hence, the five τ_4 parameters define chemical SRO by means of the simplest three-dimensional clusters.

The dependence of the $\tau_4(n)$ parameters on composition is displayed in Fig. 9, sampled in the liquid state at 1250 K for about 20 configurations taken from the sequence of isothermal runs. Within the given errorbars, derived from this averaging, we do not find significant differences between the SRO as measured by $\tau_4(n)$ parameters at different temperatures between the high temperature melt, the supercooled state, and the glassy state. That is, upon cooling there does not occur a significant increase of chemical ordering measured within the level of accuracy of our simulations. Thus, the $\tau_4(n)$ parameters are measures to characterize the amorphous packing of the alloys. From Fig. 9 we propose a sequence of differently ordered amorphous structures in the composition range with a break-down as type I for $x > 75$ atomic percentage of Zr and type II for $x < 20$ atomic percentage of Zr. Additionally, we distinguish in the middle of the composition range: type III for $65 > x > 35$ atomic percentage of Zr.

Roughly, type I is a structure dominated by $\mathrm{Co}_1\mathrm{Zr}_3$ and Zr_4 clusters, type II is dominated by $\mathrm{Co}_3\mathrm{Zr}_1$, and type III is dominated mainly by $\mathrm{Co}_1\mathrm{Zr}_3$ and by $\mathrm{Co}_2\mathrm{Zr}_2$. For $20 < x < 35$ the parameter $\tau_4(2)$ peaks. Hafner and co-workers note in their work about the magnetism of amorphous CoZr alloys [24], that the simulated alloy structures in this range of composition show large fluctuations of the SRO and, correspondingly, of the local magnetic moments. An analysis of the clusters, which are built by a Zr center atom and its nearest-neighbor shell [37], shows that alloys with $20 < x < 35$ contain only types of such clusters which are either present in structure II or in structure III. Thus, we propose to describe the corresponding total structure of the amorphous alloys with $20 < x < 35$ as a superposition of structure II and structure III.

In terms of our description, structure type I and type II may be seen as extended solution ranges, where single atoms of the respective minority component are placed in an amorphous matrix of the majority component. Type III displays a variety of different nearest-neighbor shells and resembles a smoothly varying sequence of amorphous structures, analogous to a sequence of alloy crystals.

IV. DISCUSSION

With the description of the different packings in the amorphous alloys, we may interpret the trends in the component diffusivities close to T_c. In the alloys with low contents of

Zr, i.e., essentially in type II structure, the larger Zr atoms are less mobile than the surrounding majority of Co atoms. The more Zr in the structure the denser and stiffer becomes the Zr substructure. The Zr substructure provides a skeleton of the whole structure, as the Zr atoms have a strongly reduced mobility in the supercooled melt, whereas the Co atoms will adjust themselves to this more stable Zr substructure. From this observation we can understand the increase of $T_c(x)$ in the range with atomic percentage of Zr $0<x<40$. In this range, $\zeta(x)$ reaches a maximum. This can be understood as the result of two different trends: at low Zr contents, the Zr atoms are dragged along with the flow of the Co atoms, so, the movements of the two species are closely coupled. Contrary, at higher contents of Zr, the dense Zr substructure impedes the Co movements—this is the transition to the regime, which we find for structure type III for atomic percentage of Zr $x>40$. In between these two regimes, with a sufficiently open, yet stable, Zr substructure in the alloy, the flow of Co atoms becomes relatively independent from any movements of the Zr. This maximum of ζ is reached at about $x=15$ atomic percentage of Zr, where Co diffusivity due to viscous flow is more than twenty times faster than Zr diffusivity at T_c+70 K. In the middle of the composition range $40\leqslant x<60$, i.e., for type III structure, the Co and Zr movements of the mixed amorphous structure remain closely coupled, hence ζ varies only between one and two. The transition to the alloys with high contents of Zr, $x>60$ is relatively smooth. However, here we find that the diluted Co atoms in the amorphous Zr matrix seem to act as pinning centers for the structure. Here, $\zeta<1$, so the Co atoms move only slower than the Zr atoms. We may understand this transition by considering the τ_4 statistics. We find that all structures $40\geqslant x$ are statistically dominated by Co_1Zr_3 clusters but with a decrease of the corresponding order parameter $\tau_4(3)$. The structures $x>60$ additionally contain a certain amount of tetrahedral clusters Zr_4, this is shown by $\tau_4(4)\geqslant 0$. This structure is dominated by either regions of a pure amorphous Zr packing, or single or pairs of Co atoms in the holes of this packing. Within this structure the Co atoms seem to provide the glue to hold together the whole structure. This feature is also obvious from the fact that $T_c(x)$ decreases so strongly over the whole range of composition $40>x$. Experimentally, the instability of the alloys with high contents of Zr is found in the restriction of the glass-forming ability to the range of composition with atomic percentage of Zr $x<80$ [38–40].

Our results bear some further links with experiments on glassy early-late transition-metal alloys as far one can extrapolate the behavior of the supercooled melt to the [amorphous (a-)] solid. Diffusion measurements indicate that the smaller late transition-metal atoms in amorphous alloys such as NiZr or CoZr diffuse considerably faster than Zr [41,42]. Moreover, a steep decrease of diffusivity with increasing Zr-content is found from these experimental results on a-$Co_{89}Zr_{11}$, a-$Co_{86}Zr_{14}$, and a-$Co_{81}Zr_{19}$. There are results on distinct differences in the diffusion mechanisms for Co and Zr, which also depend on alloy composition. In Co-rich alloys, Co diffuses by a collective mechanism involving some ten atoms, while Zr seems to diffuse by defect-mediated single-atom jumps [43,44]. In Zr-rich metal glasses, however, there seem to dominate defect-mediated jumps [45,46], which involves several atoms [47]. We suggest that these different diffusion mechanisms found in experiments are related to the distinct differences of the static amorphous packing at different compositions as described by our simulation data. These different packings are robust outcomes of the steric constraints in the binary metallic systems. There are also experimental results which corroborate our description regarding the particular nature of the amorphous structures in the range of composition with atomic percentage of Zr $20<x<35$, i.e., between structure type I and type III. In this range, several experiments report the presence of an amorphous phase separation. Evidence for a two-phase region between two amorphous phases was found from interdiffusion experiments on multilayers of amorphous CoZr alloys [48,49], from field-ion investigations on amorphous interlayers between Co and Zr layers [50] and from electromotive force measurements [51]. From a CALPHAD-method analysis of the metastable thermodynamics for the Co-Zr system, Gärtner *et al.* find a two-phase field in the interval between 23 and 37 atomic percentage of Zr between two amorphous phases [51]. The results by Turek *et al.* [24] on large fluctuations of the calculated magnetic moments in this range of composition for simulated amorphous CoZr also agrees with our description of these alloys as superposition of two different types of short-range ordered amorphous packings. The experiments on phase separation take place on time-scales several orders of magnitude longer than any feasible MD-simulation times (minutes to hours) and at temperatures below glass transition. This indicates that the driving forces for the phase separation in the amorphous state are weak so that it cannot be easily simulated by available MD methods and computational resources.

Finally, we note that the variation of the critical temperatures $T_c(x)$ of the simulated supercooled CoZr alloys resembles the variation of the experimental stability limit of the liquid alloys in the *equilibrium* phase diagram of the Co-Zr system [52]. In the range of compositions between the two deep eutectic points at ($x=9.5$, $T=1505$ K) and at ($x=78.5$, $T=1254$ K), the liquidus temperature $T_L(x)$ shows a strong variation with a maximum at about ($x=33$, $T=1875$ K). Clearly, due to the underlying intermetallic phases and miscibility gaps, $T_L(x)$ displays more structure than $T_c(x)$. However, in this range of composition, the simulated $T_c(x)$ values are consistently lower by a factor between 0.6 and 0.7 than the corresponding experimental $T_L(x)$, while the two curves have essentially the same shape. We take this as a further indication that the simulation model provides a realistic description of the alloy system. The correspondence between $T_L(x)$ and $T_c(x)$ suggests a link between high-temperature stability of the crystalline alloy phases and low atomic mobilities in supercooled melts with similar composition. Experiments on the atomic mobilities in these metallic alloy melts at low temperatures would be desirable to establish this correspondence between liquid dynamics and thermodynamic stability of the liquids. Qualitatively, such a correspondence could be explained by the strong interactions between Co and Zr atoms, which stabilize the crystalline alloy phases. If there are similarities between mixed clusters in the supercooled melts and the structure of the crystalline phases their strong interactions may also cause a slowing down of the dynamics of the corresponding

supercooled melts at higher temperatures than in melts with other concentrations, especially those of the two deep eutectics.

V. CONCLUSION

We have presented a simulation study on the slowing down of the diffusivities in the supercooled liquids of a glass-forming metallic binary alloy for the complete range of composition. Our finding of a huge variation of the critical temperature $T_c(x)$ over 500 K is a rather unexpected result. The approximate scaling of the lines of constant mobilities $D(x;T-T_c(x))$ indicates a close relation between the atomic mobilities and the glass-transition temperature, irrespective of structural differences and differences of the component mobilities between supercooled alloys. Roughly, we find T_c at about 100 K below the temperatures, where $D(x) = 10^{-6}$ cm^2/s in our simulation data. However, the behavior of the ratio of the component diffusivities reflects differences in the structure of the different alloys. This was demonstrated by the apparent interrelation between this ratio for the different alloys and the τ_4 order parameters, which measure the chemical SRO in terms of the probabilities for finding differently composed tetrahedral clusters in the supercooled alloys.

[1] J. Jäckle, Rep. Prog. Phys. **49**, 171 (1986).
[2] E. Leutheusser, Phys. Rev. A **29**, 2765 (1984).
[3] U. Bengtzelius, W. Götze, and A. Sjölander, J. Phys. C **17**, 5915 (1984).
[4] W. Götze, in *Liquids, Freezing, and Glass Transition*, edited by J.P. Hansen, D. Levesque, and J. Zinn-Justin (North-Holland, Amsterdam, 1991).
[5] W. Götze and L. Sjögren, Rep. Prog. Phys. **55**, 241 (1992).
[6] J.-L. Barrat and A. Latz, J. Phys.: Condens. Matter **2**, 4289 (1990).
[7] M. Fuchs, I. Hofacker, and A. Latz, Phys. Rev. A **45**, 898 (1992); M. Fuchs, W. Götze, S. Hildebrand, and A. Latz, Z. Phys. B: Condens. Matter **87**, 43 (1992).
[8] J. Bosse and Y. Kaneko, Phys. Rev. Lett. **74**, 4023 (1995).
[9] U. Bengtzelius, Phys. Rev. A **33**, 3433 (1986).
[10] M. Nauroth and W. Kob, Phys. Rev. E **55**, 657 (1997).
[11] R. Schilling and T. Scheidsteger, Phys. Rev. E **56**, 2932 (1997).
[12] S. Kämmerer, W. Kob, and R. Schilling, Phys. Rev. E **56**, 5450 (1997).
[13] T. Franosch, W. Götze, M.R. Mayr, and A.P. Singh, Phys. Rev. E **56**, 5659 (1997).
[14] T. Franosch, W. Götze, J. Phys.: Condens. Matter **6**, 4807 (1994).
[15] K. Kawasaki, Physica A **243**, 25 (1997).
[16] A. Inoue, T. Zhang, and T. Masumoto, J. Non-Cryst. Solids **150**, 396 (1992).
[17] A. Peker and W.L. Johnson, Appl. Phys. Lett. **63**, 2342 (1993).
[18] A. Inoue, T. Zhang, and T. Masumoto, J. Non-Cryst. Solids **156-158**, 473 (1993).
[19] For a recent survey, see, e.g., R. Busch, E. Bakke, and W.L. Johnson, in *Synthesis and Properties of Mechanically Alloyed and Nanocrystalline Materials - ISMANAM 96*, Vol. 235-238 of Materials Science Forum, edited by D. Fiorani (Transtec Publications, Zürich-Uetikon, 1997), p. 327, and further papers there.
[20] See, e.g., P. Lamparter and S. Steeb, in *Materials Science and Technology*, edited by R.W. Cahn, P. Haasen, and E.J. Kramer (VCH, Weinheim, 1994), Vol. 1, p. 217, and references therein.
[21] Ch. Hausleitner and J. Hafner, J. Phys.: Condens. Matter **2**, 6651 (1990).
[22] Ch. Hausleitner and J. Hafner, Phys. Rev. B **45**, 115 (1992); **45**, 128 (1992).
[23] Ch. Hausleitner and J. Hafner, J. Non-Cryst. Solids **144**, 175 (1992).
[24] I. Turek, Ch. Becker, and J. Hafner, J. Phys.: Condens. Matter **4**, 7257 (1992).
[25] C.W. Gear, *Numerical Initial Value Problems in Ordinary Differential Equations* (Prentice-Hall, Englewood Cliffs, NJ, 1971).
[26] F.R. de Boer, R. Boom, W.C.M. Mattens, A.R. Miedema, and A.K. Niessen, *Cohesion in Metals. Transition Metal Alloys* (North-Holland, Amsterdam, 1988).
[27] M. Steyer, H.-U. Krebs, and H.C. Freyhardt, J. Non-Cryst. Solids **66**, 317 (1987).
[28] Yu. A. Babanov, A.F. Sidorenko, Z.V. Ryazhkin, V.R. Shvestov, J. Moessinger, and H. Kronmueller, Nucl. Instrum. Methods Phys. Res. A **405**, 400 (1998).
[29] L.V. Woodcock and C.A. Angell, Phys. Rev. Lett. **47**, 1129 (1989).
[30] J. Matsui, T. Odagaki, and Y. Hiwatari, Phys. Rev. Lett. **73**, 2452 (1994).
[31] H. Teichler, Phys. Rev. Lett. **76**, 62 (1996).
[32] H. Teichler, Phys. Rev. E **55**, R4287 (1996).
[33] L.J. Lewis, Mater. Sci. Eng., A **133**, 423 (1991).
[34] G. Wahnström, Phys. Rev. A **44**, 3752 (1991).
[35] W. Kob and H.C. Andersen, Phys. Rev. E **51**, 4626 (1995).
[36] J. Baschnagel, Phys. Rev. B **49**, 135 (1994).
[37] U.K. Rößler, Thesis, Universität Göttingen, 1995.
[38] J. Eckert, L. Schultz, and K. Urban, J. Less-Common Met. **145**, 283 (1988).
[39] A. Regenbrecht, G. v. Minnigerode, and K. Samwer, Z. Phys. B: Condens. Matter **79**, 25 (1990).
[40] R.M. Idrus and P.J. Grundy, Z. Phys. B: Condens. Matter **92**, 17 (1993).
[41] W. Dörner and H. Mehrer, Phys. Rev. B **44**, 101 (1991).
[42] A. Heesemann, K. Rätzke, and F. Faupel, Europhys. Lett. **29**, 221 (1995).
[43] P. Klugkist, K. Rätzke, S. Rehders, P. Troche, and F. Faupel, Phys. Rev. Lett. **80**, 3288 (1998).
[44] P. Klugkist, K. Rätzke, and F. Faupel, Phys. Rev. Lett. **81**, 614 (1998).
[45] A. Grandjean, P. Blanchard, and Y. Limoge, Phys. Rev. Lett. **78**, 697 (1997).
[46] H.J. Höfler, R.S. Averback, G. Rummel, and H. Mehrer, Philos. Mag. Lett. **55**, 301 (1992).
[47] K. Rätzke, P. Klugkist, and F. Faupel, Defect Diffus. Forum **65**, 43 (1999).

[48] F. Stobiecki, T. Stobiecki, and H. Hoffman, in *Procedings of the 12th International Colloquium on Magnetic Films and Surfaces* (Sociéte Française du Vide, Paris, 1988), Thp-26.
[49] F. Stobiecki, T. Stobiecki, H. Hoffman, J. Dubowik, and Y.V. Kudryatvtsev, Thin Solid Films **174**, 45 (1989).
[50] R. Busch, F. Gärtner, S. Schneider, R. Bormann, and P. Haasen, in *Polycrystalline Thin Films: Structure, Texture, Properties and Applications*, Materials Research Society Symposium Proceedings No. 343 (Materials Research Society, Pittsburgh, 1994), p. 229.
[51] F. Gärtner, C. Michaelsen, and R. Bormann, Philos. Mag. B **76**, 511 (1997).
[52] *Binary Alloy Phase Diagrams*, edited by T.B. Massalski (ASM International, Metals Park, Ohio, 1990), p. 1265.